

Corotating interaction region (CIR) induced magnetic storms during solar minimum and their effects on low-latitude geomagnetic field and ionosphere

B Veenadhari^{1,§,*}, Sandeep Kumar¹, S Tulasi Ram², Rajesh Singh³ & S Alex¹

¹Indian Institute of Geomagnetism, New Panvel, Navi Mumbai 410 218, India

²EGRL, Indian Institute of Geomagnetism, Tirunelveli 627 011, India

³KSK Geomagnetic Research Laboratory, IIG, Chamanganj, Allahabad 221 505, India

[§]E-mail: bveena@iigs.iigm.res.in

Received October 2011; accepted 23 February 2012

The corotating interaction region (CIR) induced magnetic storms which occurred during solar minimum are investigated to study their effects on equatorial and low-latitude ionosphere and geomagnetic field at Indian sector. This work was a part of Indian CAUSES campaign for the period of March – April 2006. The penetration electric fields play a crucial role in modifying equatorial electric fields during severe magnetic storms and these effects are not studied in detail for moderate magnetic storm originated by CIRs. The present paper investigates the effects of CIR related moderate storms and found that during the moderate magnetic storms, the short lived (duration of 2 - 3 h) penetration of high latitude electric fields to equatorial ionosphere exists during local morning and noon hours during main phase as inferred from changes in EEJ with the response to interplanetary electric field. The variations of EEJ are linearly correlated with the sudden changes in interplanetary electric field (IEF_y) around morning to noon hours, which confirms existence of the penetration of electric fields.

Keywords: Geomagnetic storm, Corotating interaction region (CIR), Interplanetary electric field, Equatorial electrojet (EEJ) strength, Penetration electric field, F-region critical frequency

PACS Nos: 94.30.Lr; 96.60.qd

1 Introduction

During solar maximum, the Sun's activity is dominated by flares and erupting filaments, and their associated coronal mass ejections (CMEs). The predominance of CMEs and interplanetary magnetic field (IMF) conditions cause the development of geoeffective magnetic storms during solar maximum. Large magnetic storms are often associated with CMEs that cause the sudden and large disturbances in magnetosphere and ionosphere. The prime condition of intense magnetic storms ($Dst < -100$ nT) is the occurrence of intense (IMF $B_z < \sim -10$ nT) and long duration ($\Delta t \sim 3$ h or longer) southward interplanetary magnetic fields, allowing a more effective energy transfer between solar wind and magnetosphere through magnetic reconnection mechanism¹⁻⁴. The CME driven shocks and magnetic storms occur frequently during solar maximum, when the solar activity is high. A number of investigations are carried out on CME driven magnetic storms during the last two solar cycles and the results have identified their solar and interplanetary sources⁵⁻⁸. The effect of

intense magnetic storms on ionosphere is also thoroughly examined for different latitudes and their spatial and temporal characteristics are fairly understood⁹⁻¹⁰. The basic storm time mechanisms like penetrating of interplanetary electric fields from high latitude to equator and disturbance dynamo of equator ward winds during intense magnetic storms are well investigated¹¹⁻¹³ using ground based and radar data and estimated efficiency of electric fields and model simulations¹⁴⁻¹⁶.

During solar minimum period or descending phase of solar cycle, the high speed solar wind streams from coronal holes (CHs) plays a major role in the generation of moderate geomagnetic storms under different IMF conditions. Solar activity and topology of heliospheric current sheet (HCS) are highly dependent on different phases of solar cycle. During solar minimum, the sun's streamer belts are confined to the region around the heliographic equator and corotating high speed solar stream is associated with equator ward extended coronal holes. When high speed solar wind streams (HSS) emanating from

coronal holes interact with streams of lower speed, a solar wind structure called a corotating interaction region (CIR) is developed, leading to intense magnetic field¹⁷. CIRs can result in recurrent geomagnetic storms whose period is equal to the rotational rate of the sun ~27 days^{18,19}. IMF Bz fluctuations within CIRs causes magnetic reconnection with the Earth's magnetic fields, allowing transfer of solar wind energy to the magnetosphere and generate weak to moderate intensity magnetic storms²⁰. However, the CIR induced geomagnetic storms are paid less attention partly due to their less to moderate level of intensities. The CIR storms also produce similar changes to those associated with isolated geomagnetic storms, however, with smaller amplitudes²¹. Further, CIR storms appear recurrently producing recurrent geomagnetic and ionospheric perturbations. Tsurutani & Gonzalez²² defined the High-Intensity, Long-duration, Continuous AE activity (HILDCAA) interval events that occurred during high speed solar wind streams. The HILDCAA events have certain characteristics with AE peak values exceeding 1000 nT with a duration of minimum 2 days, which causes moderate to minor magnetic storms²³. It is also shown that the total energy input to the Earth's magnetosphere can be larger during solar declining phase intervals versus solar maximum intervals because of continuous, though weak external forcing^{24,25}. Thus, it gained interest to study the phenomena occurring during solar minimum conditions. Some studies are carried out on CIR driven moderate magnetic storms and their properties during declining phase and minimum of solar cycle 23 (Ref 26). But the effects of CIR driven magnetic storms and HILDCAA events on ionosphere are not given proper attention and not investigated widely. Recent studies indicate that both the geomagnetic activity and ionosphere-thermosphere system undergo periodic modulation at sub-harmonic solar rotational periodicities (13.5 and 9-day) due to recurrent CIRs²⁷⁻²⁹. Further, they have also reported that the CH area on the Sun and solar wind velocity exhibit greater tendency for sub-harmonic periodicities during the extreme solar minimum year 2008 and shown that both day and night side ionospheric electron density undergo coherent oscillations with SW and Kp. However, the modifications in the ionospheric electric fields and associated changes in electron density during the CIR-HILDCAA events are poorly understood. Studies on few HILDCAA events

indicate marginal effects due to disturbance dynamo electric fields, however, no clear signatures of prompt penetration electric fields are identified³⁰. Recently, CH interval of 25 March to 26 April, is examined with the response of vertical total electron content (VTEC) and found that VTEC intensifies during HSS periods and largest variations are noticed in low latitudes VTEC (Ref 31) (between -30° and 30°) and suggested that CIRs/HSS are external drivers for both thermospheric and ionospheric phenomena during sunspot minimum³¹.

The solar cycle 23 ended in 2006 but the prolonged solar minimum is continued up to the end of the year 2008. In the solar minimum year 2006, a coordinated multi-instrument campaign mode observations were carried out during March – May 2006 under CAWSES India program which provided a unique opportunity to study the response of ionosphere to the forces coupled from lower atmosphere as well as of solar and interplanetary origin. Indian Institute of Geomagnetism (IIG), India has participated in CAWSES campaign and magnetic variations were recorded at all geomagnetic observatories with high resolution of data. As solar minimum was reached during 2006, a few moderate magnetic storms are occurred due to high speed solar wind streams with CIRs and the low and equatorial geomagnetic activity varied from moderate to severe disturbed conditions with rapid fluctuations in interplanetary parameters. The present study focuses on the effects of CIR related storms on equatorial electrodynamics with special emphasis to identify the signatures associated with the ionospheric electric fields in the equatorial electrojet variations and study the importance of their time scales and local time dependency. The ionospheric response for CIR related magnetic storms is also discussed using ionosonde data from equatorial station Trivandrum.

2 Data

The digital ground magnetic data of H component with one minute time resolution are taken from the Indian equatorial station, Tirunelveli (TIR: geomagnetic latitude 0.06°N, longitude 150.55°E) and the low latitude station, Alibag (ABG: geomagnetic latitude 10.32°N, longitude 146.67° E). The TIR station is convenient to monitor the equatorial electrojet (EEJ), while the ABG is located outside its influence. The simultaneous data obtained from these two stations are thus, well suited for estimating

the strength of the equatorial electrojet. The EEJ index is computed by the difference between ΔH (TIR) and ΔH (ABG). ΔH is the departure from the nighttime base value for the H component. Geo-effectiveness of disturbance characteristics is dealt in by monitoring the variation in the H component of the magnetic field at TIR and ABG during magnetic storm periods. The solar wind and other interplanetary parameters are obtained from the Advanced Composition Explorer (ACE) spacecraft, positioned at about 224 RE. The geomagnetic activity data such as AE, Kp and Sym-H-indices are obtained from World Data Center for Geomagnetism, Kyoto University (<http://wdc.kugi.kyoto-u.ac.jp/>). One min resolution data from ground and satellite has been used to study the detailed causes of CIR storms with southward Bz variations. During the campaign period (March – May 2006), the ionosonde measurements were carried out at equatorial station Trivandrum with interval of 5 min. The good resolution data is used to identify the penetrating electric fields during the storm periods.

3 Results and Discussion

3.1 CIR originated magnetic storms

A series of geomagnetic storms of moderate intensity (with peak negative Sym-H ≤ -50 to -100 nT) have been observed during the 3-month CAUSES India campaign period from March to May 2006. Figure 1 illustrates the interplanetary solar wind and geomagnetic activity parameters for the period March to May 2006. The top to bottom panels show interplanetary magnetic field magnitude (|B_i|); SW proton velocity (V_p); temperature (T_p); density (N_p); z-component of interplanetary magnetic field (IMF B_z); AE index; Kp index; and Sym-H index, respectively as a function of day number from March to May 2006, when solar minimum was in progress. The most striking features that can be noticed is a series of enhanced solar wind magnetic field (|B_i|) and density (N_p) structures [Figs 1(a and d)] impinging on geospace environment leading to a series of geomagnetic disturbances. The solar wind velocity (V_p) and temperature (T_p) also exhibit concurrent

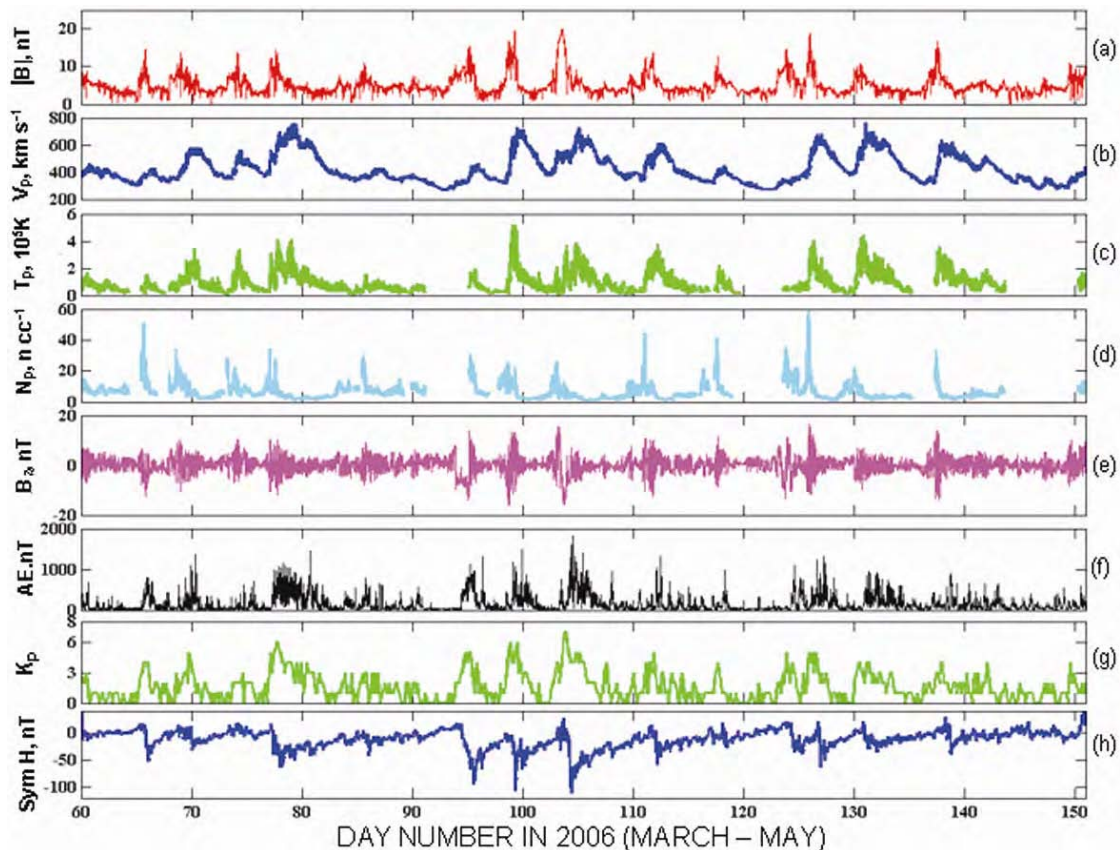


Fig. 1 — Recurrent geomagnetic storms associated with HSS-CIR structures in low solar activity year 2006; Panels from top to bottom show the variations of: (a) solar wind magnetic field strength (|B_i|); (b) proton bulk velocity (V_p); (c) temperature (T_p); (d) density (N_p); (e) IMF B_z; (f) AE -index; (g) K_p index; and (h) Sym-H index as a function of day number in 2006

enhancements [Figs 1(b and c)] with enhancements in solar wind magnetic field strength ($|B|$). From a careful examination of Figs 1(a-d), one can notice that the solar wind density (N_p) exhibits impulse type enhancements simultaneously with $|B|$, however, followed by sudden drops while the solar wind velocity (V_p) and temperature (T_p) are still increasing or remain at high state. These are the typical features of CIR interface regions^{20,27}. Further, the IMF B_z also exhibits fast positive and negative excursions around these regions, and the negative excursions of which enables magnetic reconnection and causes geomagnetic activity as can be observed from the variations of AE, Kp and Sym-H indices [Figs 1(f-h)]. However, because of the oscillatory nature of IMF B_z , the resultant geomagnetic storms are typically of only weak to moderate intensity³². From the variation of Sym-H index [Fig. 1(h)], it can be clearly seen that there were a series of CIR induced geomagnetic storms of moderate intensity (~ -100 to -50 nT) during this campaign period. Though many of these storms have been investigated, only the results during two typical CIR storm events are presented in

this paper to describe the characteristics of CIRs and their effects on equatorial geomagnetic field and ionospheric variations.

3.1.1 Magnetic storm of 18-19 March 2006

Figure 2 shows an example of CIR generated magnetic storm of 18-19 March 2006. This is a gradual commencement (GC) storm, which commenced at 03:00 hrs UT on 18 March and ended at 23:00 hrs UT on 20 March 2006. This storm resulted from a corotating interaction region preceding a high speed stream from the coronal hole on early 17 March. The top four panels show the solar wind density (N_p); solar wind speed (V_{sw}); Proton temperature (T_p); and IMF B_z along with Sym-H variation in Fig. 2(e). On 18 March, solar wind speed was slow with 400 km s^{-1} up to 09:00 hrs UT and rose to 580 km s^{-1} and continued for several hours before it reached 700 km s^{-1} on 19 March. The first rise in solar wind speed at around 08:30 hrs UT was associated with simultaneous enhancement in proton temperature (T_p). However, the solar wind proton density (N_p) exhibited a sudden drop at the same. This signifies

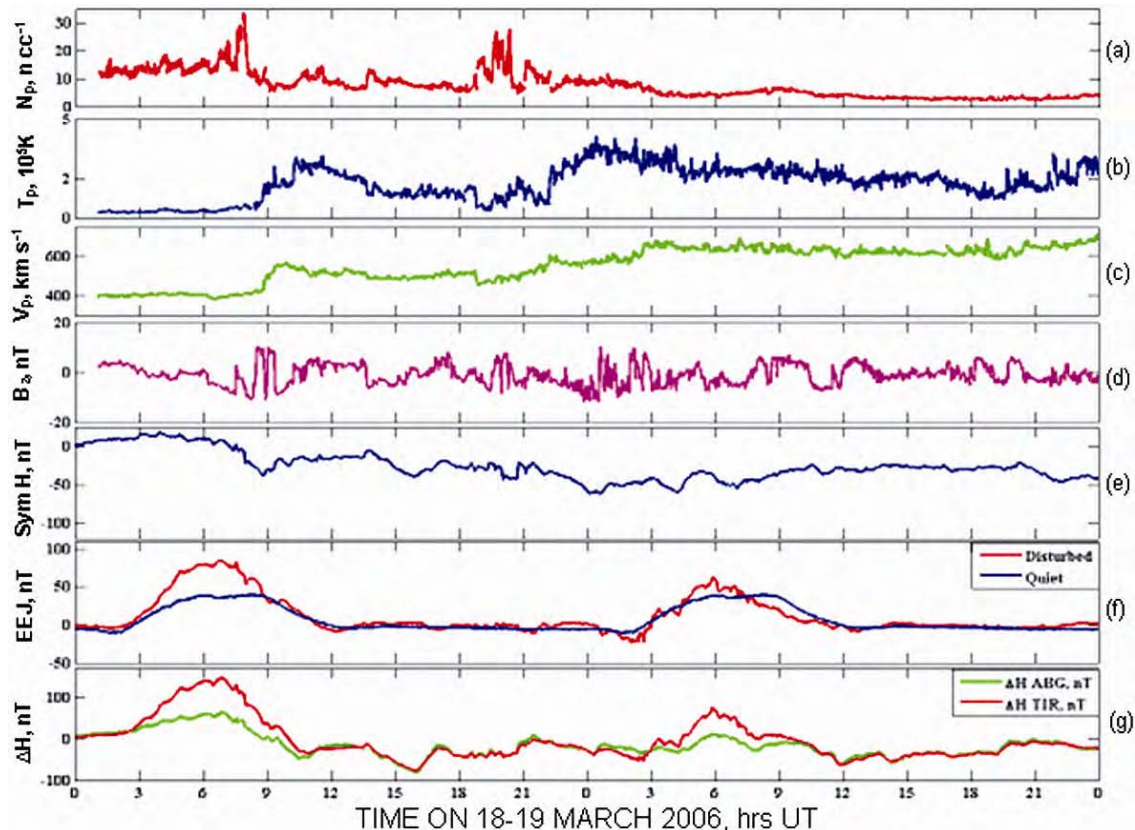


Fig. 2 — CIR generated magnetic storm of 18 – 19 March 2006: (a) Proton density (N_p); (b) Temperature (T_p); (c) SW velocity (V_p); (d) IMF B_z ; (e) Sym-H; (f) Equatorial electrojet strength (EEJ); (g) H component data from TIR and ABG stations

the interaction between the two streams and can be noted by the increase in T_p . From Fig. 2, the positive increase in Sym-H is also noted from 00:00 to 06:00 hrs UT and this occurs when proton density enhancement impacts the magnetosphere. The ram pressure increase associated with this high density and low velocity plasma compresses the magnetosphere and causes an increase in horizontal field strength at the surface of the earth. These are the typical features of the CIR stream interface region and different interplanetary phenomena than the CME associated storms. The IMF Bz exhibits positive and negative fluctuations during this period, probably, associated with Alfvén waves within the CIRs³³. The low latitude geomagnetic field ranged from quiet to moderate levels. In Fig. 2(g), the storm time variation of ΔH (TIR) and ΔH (ABG) are shown and the EEJ computed for storm time and compared with quiet EEJ variation [Fig. 2(f)]. The time shift of ~ 61 min is adjusted for ACE parameters to match with ground magnetic data. The storm time EEJ shows significant enhancement during 03:00 – 09:00 hrs UT (08:30 – 14:30 hrs LT) of 18 March when compared to the

quiet time EEJ variation. This period is considered to examine the signatures of prompt penetration electric fields (PPEFs) in the EEJ variation.

3.1.2 Magnetic storm of 9-10 April 2006

The moderate magnetic storm of 9-10 April 2006 (Fig. 3), which commenced at 00:00 hrs UT on 9 April 2006, was due to the presence of geo-effective coronal hole wind stream of 7 April 2006. On 9 April, the enhancement in N_p , during initial phase of the storm, was associated with large negative excursions in IMF Bz while the solar wind velocity and temperature were at low levels up to 06:00 hrs UT. After that, the sudden increase in T_p and V_p were associated with sudden decrease in N_p which clearly signifies the interaction of slow and fast streams of CIR regions. Highly fluctuating pattern was seen in the IMF Bz component and sustained for the entire duration of storm. The V_p and T_p sustained for higher levels for long time during recovery phase of the storm that coincided with the fast positive and negative excursions in IMF Bz which are the signatures of Alfvénic waves in CIRs (Ref. 22). As

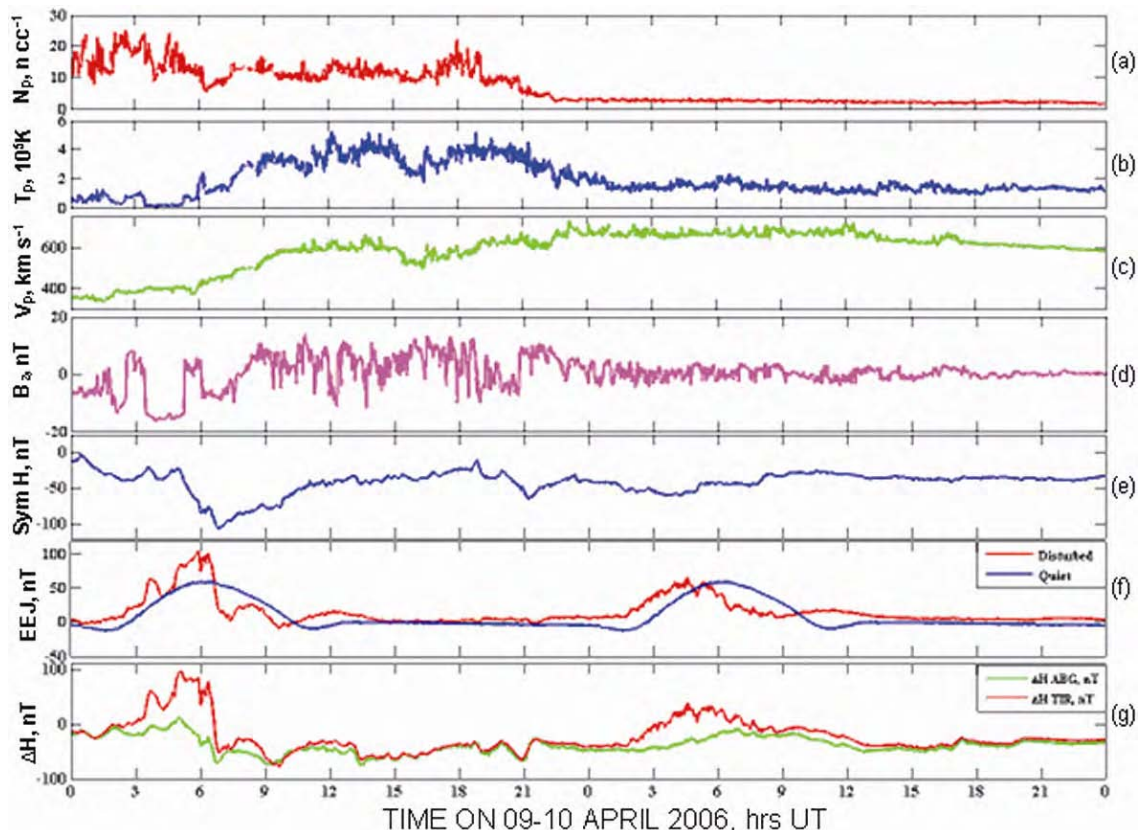


Fig. 3 — Moderate magnetic storm of 9-10 April 2006: (a) Proton density (N_p); (b) Temperature (T_p); (c) SW velocity (V_p); (d) IMF Bz; (e) Sym-H; (f) Equatorial electrojet strength (EEJ); (g) H component data from TIR and ABG stations

the recovery of the storm progressed, though these fluctuations minimized on 10 April but the solar wind speed remained steady at $\sim 600 \text{ km s}^{-1}$. The time shift of 50 min was adjusted for ACE parameters. During the period of geomagnetic activity, variations in the ΔH component at TIR and ABG showed modulating pattern simultaneously with the interplanetary components. The maximum negative excursion in Sym-H was about -100 nT at about 07:00 hrs UT on 9 April and tended to recover but remained with lower values for the entire storm period [Fig. 3(f)]. The EEJ for storm time and quiet period is computed and shown in Fig. 3(g). It is important to note that the long negative excursion of about -19 nT in IMF Bz on 19 April during 03:00 – 06:00 hrs UT well coincided with the increase in EEJ strength which showed the strengthening of day time eastward electric field. The EEJ variations implied the electric field changes at equatorial station which also altered the equatorial $E \times B$ drifts. The above mentioned two moderate magnetic storms were selected to study the variations in PPEFs because the EEJ variations indicated strong eastward/westward electric fields during local morning and noon hours which were well coincided

with variations in IMF Bz during the main phase of CIR storms.

3.2 Short lived penetration electric field events

The dawn-to-dusk component of interplanetary electric field ($IEF_Y = -V_{sw} \times B_z$) is computed from the interplanetary solar wind parameters observed by Atmospheric Composition Explorer (ACE) at L1-point. The solar wind and IEF_Y parameters have been shifted to account for the delay from ACE location to the bow shock (<http://omniweb.gsfc.nasa.gov/html/HROdocum.html>). The response in equatorial electrojet (EEJ) strength for the sharp changes in interplanetary electric field (IEF_Y) is examined from the ground based magnetometer data at TIR and ABG. In order to filter out the background diurnal (local time) variation in EEJ strength, the ΔEEJ is computed by subtracting the geo-magnetically quiet day variation of EEJ strength. Two typical examples of direct penetration of IEF_Y to equatorial ionosphere as inferred by the corresponding changes in the EEJ strength during two CIR driven geomagnetic storms on 18 March 2006 and 09 April 2006 are presented in Fig. 4. The top panels of Fig. 4 show the variations in

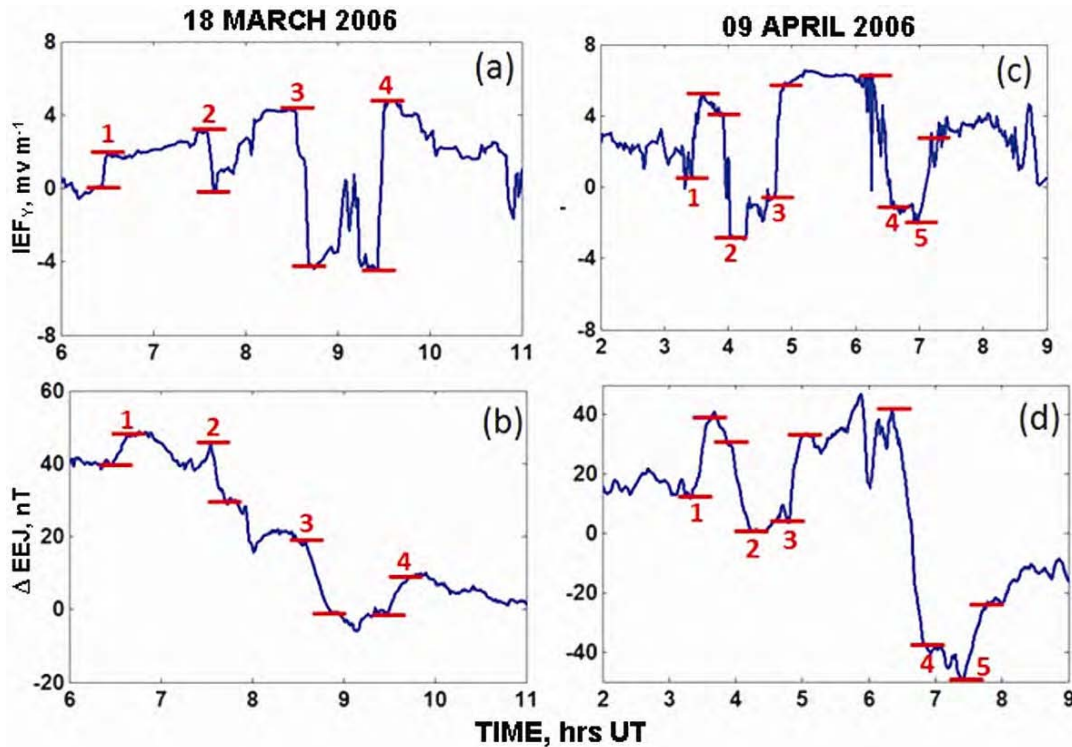


Fig. 4 — Direct influence of interplanetary electric field (IEF_Y) on the equatorial electric field as inferred by the changes in equatorial electrojet (EEJ) strength (top panels show the changes in IEF_Y and the bottom panels show the corresponding changes in ΔEEJ ; the identified sharp changes in IEF_Y and ΔEEJ are marked by numbers 1,2,3... are considered to estimate a statistical relationship between changes IEF_Y and ΔEEJ)

IEF_Y and the bottom panels show the corresponding changes in Δ EEJ. The data pertaining to the main phase of storm only are presented here for better visibility of the sharp variations in IEF_Y and Δ EEJ. It can be observed from these figures, the Δ EEJ strength [Figs 4(b and d)] which is a proxy of zonal electric field at equatorial latitudes exhibit corresponding changes in response to sharp changes in the interplanetary electric field (IEF_Y) [Figs 4(a and c)]. In order to estimate a quantitative relationship between the changes in IEF_Y and Δ EEJ, only sharp changes in IEF_Y as marked by numbers 1,2,3... in Fig. 4 have been considered. It can be observed from Fig. 4 that whenever the IEF_Y exhibit a sharp increase, the corresponding Δ EEJ also exhibit sharp increase [at 1, 4 in Figs 4(a,b) and at 1,3,5 in Figs 4(c,d)]. Similarly, Δ EEJ exhibit sharp decrease when the IEF_Y exhibit sudden decrease [at 2,3 in Figs 4(a,b) and at 2,4 in Figs 4(c,d)].

The statistical relationship between the changes in IEF_Y and Δ EEJ is presented in Fig. 5. The horizontal axis represents the net change in the IEF_Y and the vertical axis represents the net change in the Δ EEJ. It can be clearly observed from Fig. 5 that there exists a linear relationship between the changes in IEF_Y and Δ EEJ. The positive/negative signs indicate increase/decrease in IEF_Y and Δ EEJ. The solid line in Fig. 5 represents the linear least-squares fit of the data. From the preliminary analysis of 9 cases shown in Fig. 4, the linear relationship can be expressed by the following equation:

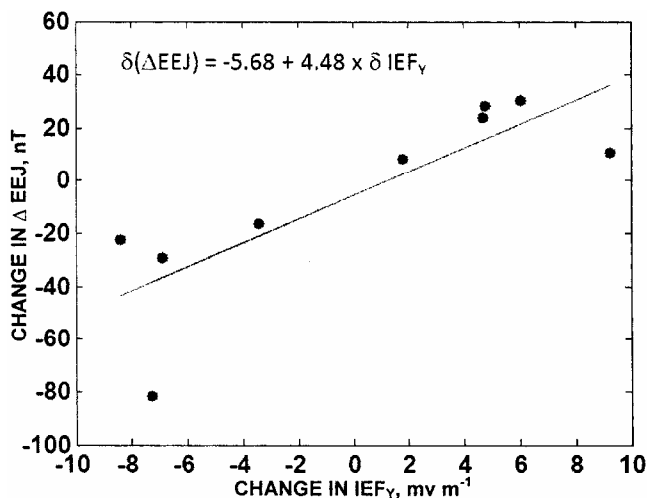


Fig. 5 — Relationship between changes in IEF_Y and Δ EEJ from a preliminary analysis of 9 cases shown in Fig. 1 (solid line represents the linear least-squares fit of the data)

$$\delta(\Delta\text{EEJ}) = -5.68 + 4.48 \times \delta \text{IEF}_Y \quad \dots(1)$$

Huang *et al.*³⁴ have also made a statistical analysis to examine the equatorial ionospheric field changes to the changes in interplanetary electric field. They have considered a total of 73 events between 10:00 and 15:00 hrs LT in which the sudden changes in the ionospheric electric fields are linearly correlated with corresponding changes in IEF. Given that the changes in EEJ primarily reflect the changes in the equatorial ionospheric electric field, the linear relationship between the changes in IEF_Y and Δ EEJ is consistent with the observations of Huang *et al.*³⁴. Generally, the linear relationship between EEJ and IEF_Y shows the existence of prompt penetration of interplanetary electric field to equatorial latitudes during the main phase of severe magnetic storms, which can be inferred from variations in H component of ground magnetic data from equatorial latitudes and from southward interplanetary magnetic field (IMF B_z) (Ref. 35). In the case of moderate magnetic storms originated by CIRs, these signatures are rarely identified in EEJ because of gradual variations in interplanetary parameters. However, in the present analysis, sharp changes in EEJ are observed during noon hours in response to the interplanetary electric field changes. Further, the efficiency of penetration electric fields depends on ionospheric conductivity which varies with local time and is maximum during local morning and noon^{15,36}. Hence, a detailed investigation for a quantitative assessment of perturbations induced in equatorial ionospheric electric field due to the changes in IEF and its local time dependency is necessary and considered for future work.

3.3 Ionospheric effects

The effects of CIR induced geomagnetic storms on F-region ionosphere are studied using 5-min resolution of ionosonde data from Indian equatorial station, Trivandrum. Figure 6 shows the variations (in red color) in ionospheric parameters foF₂ and h'F during 18-19 March and 9-10 April 2006 geomagnetic storms. The average of 5 quiet day variations is also shown to compare the disturbed day variations (in blue color). The top panels and bottom panels represent the foF₂ and h'F variations, respectively. It is noted that the foF₂ decreases from 10:00 – 16:00 hrs LT (04:30 – 10:30 hrs UT) on 18 March in response to enhanced EEJ [Fig 2(b)] during the same period. This decrease in foF₂ (2 MHz) may indicate

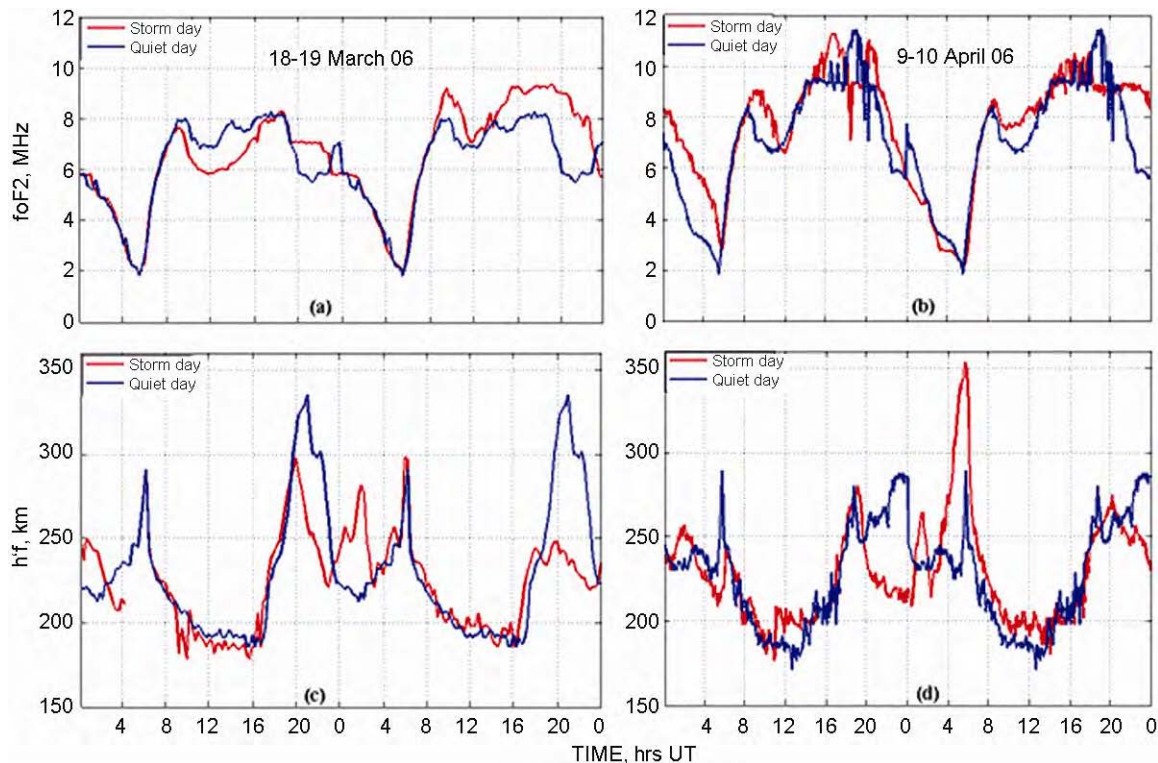


Fig. 6 — Ionospheric parameters F-region critical frequency (f_oF_2) and virtual height of base of F-layer ($h'F$) (in red color) for the two magnetic storms of 18-19 March 2006 and 9-10 April 2006 in local time (LT); Average of 5 quiet day is plotted in blue. These parameters are clearly shown to identify the effects of PPEFs for CIR magnetic storms

an enhancement in EIA with more depletion of plasma than on the quiet day at the equatorial station Trivandrum as can be seen from Fig 4(a). There is not much difference in the height, $h'F$ at the same period. On 19 March during 08:00 – 10:00 hrs LT (02:30 – 04:30 hrs UT), there is slight increase in f_oF_2 , followed by decrease. Again, it has shown enhancement after 14:00 hrs LT (08:30 hrs UT). During the same period, the EEJ variations depict the marginal decrease in EEJ during first part (02:30 – 04:30 hrs UT) and later followed by increase (Fig. 2). The variations in EEJ strength could be the cause for changes in f_oF_2 variations. Though the EEJ variations are not very significant as 18 March, but the IMF B_z shows the rapid fluctuations during the same period. The enhancement in f_oF_2 is persisted from 14:00 hrs LT (08:30 hrs UT) till night and could be attributed to pre-reversal enhancement of f_oF_2 and also the magnetic storm was in long recovery phase which is one of the characteristics of CIR storms.

In case of 9 April, the f_oF_2 increases during 09:00 – 11:00 hrs LT (03:30 – 05:30 hrs UT) in response to decrease in EEJ [Fig 4(d)], indicating

the existence of day time westward electric field that causes inhibition of EIA during initial hours. Unfortunately, the ionosonde data from other Indian low latitude stations were not available to verify the changes in f_oF_2 and confirm the EIA strengthening/inhibition. However, the earlier studies^{36,37-39} report that the decrease/increase in f_oF_2 at equatorial stations are closely associated with increase/decrease in f_oF_2 at low-latitude stations during the main phase of severe magnetic storms, which represents the EIA enhancement/inhibitions due to presence/subsidence of eastward PPEFs. Further, the present study reiterates the same signatures during the CIR generated moderate geomagnetic storms. These two case studies reveal the effect of short lived PPEFs on equatorial ionosphere and electric field signatures can be inferred from EEJ. One cannot rule out the role of disturbance dynamo which also alter the equatorial ionosphere with disturbed neutral winds and electric fields. But in these cases, the negative variations in IMF B_z indicates the dominance of PPEFS over disturbance dynamo. However, further studies are essential to examine possibilities with more number of events.

4 Summary

The tailing high speed streams and corotating interactive region originated magnetic storms are examined using Indian low and equatorial geomagnetic and ionospheric data. The low-latitude geomagnetic field varied from moderate to severe storm conditions due to CIR and associated long duration of disturbed interplanetary conditions. It is found out that during local noon, the short lived (2-3 h duration) penetrating electric field signatures are clearly seen in EEJ even during the moderate levels of geomagnetic activity induced by CIRs. The variations of EEJ are linearly correlated with the sudden changes in interplanetary electric field (IEF_V) around morning to noon hours; however, the expected local time dependency on efficiency of penetration of electric fields needs further investigation.

Acknowledgements

The authors are thankful to the support provided by ISRO in the CAWSES India campaign program.

References

- Dungey J W, Interplanetary magnetic field and the auroral zones, *Phys Rev Lett (USA)*, 6 (1961) 47.
- Gonzalez W D, Joselyn J A, Kamide Y, Kroehl H W, Rostoker G, Tsurutani B T & Vasyliunas V M, What is a geomagnetic storm?, *J Geophys Res (USA)*, 99 (1994) pp 5771–5792.
- Gonzalez W D, Tsurutani B T & Clua de Gonzalez A L C, Interplanetary origin of geomagnetic storms, *Space Sci Rev (Netherlands)*, 88 (1999) pp 529–562.
- Webb D F, Cliver E W, Crooker N U, Cyr O C St & Thompson B J, Relationship of halo coronal mass ejections, magnetic clouds, and magnetic storms, *J Geophys Res (USA)*, 105 (2000) pp 7491–7508.
- Zhang J, Richardson I G, Webb D F, Gopalswamy N, Huttunen E, Kasper J C, Nitta N V, Poomvises W, Thompson B J, Wu C -C, Yashiro S & Zhukov A N, Solar and interplanetary sources of major geomagnetic storms (Dst \geq 100 nT) during 1996–2005, *J Geophys Res (USA)*, 112 (2007) A10102.
- Gopalswamy N, Lara A, Lepping R P, Kaiser M L, Berdichevsky D & Cyr O C St, Interplanetary acceleration of coronal mass ejections, *Geophys Res Lett (USA)*, 27 (2000) pp 145–148.
- Gonzalez W D, Tsurutani B T, Lepping R P & Schwenn, Interplanetary phenomenon associated with very intense geomagnetic storms, *J Atmos Terr Phys (UK)*, 64 (2002) pp 173–181.
- Tsurutani B T & Gonzalez W D, The future of geomagnetic storm predictions: implications from recent solar and interplanetary observations, *J Atmos Terr Phys (UK)*, 57 (1995) 1369.
- Rastogi R G & Patel V L, Effect of interplanetary magnetic field on ionosphere over the magnetic equator, *Proc Indian Acad Sci*, 82 (1975) pp 121–141.
- Reddy C A, Somayajulu V V & Viswanathan K S, Backscatter radar measurements of storm time electric fields changes in the equatorial electrojet, *J Atmos Terr Phys (UK)*, 43 (1981) pp 817–827.
- Kelley M C, Fejer B G & Gonzalez C A, An explanation for anomalous equatorial ionospheric electric field associated with a northward turning of the interplanetary magnetic field, *Geophys Res Lett (USA)*, 6 (1979) 301.
- Fejer B G, Gonzalez C A, Farley D T, Kelley M C & Woodman R F, Equatorial electric fields during magnetically disturbed conditions 1: The effect of interplanetary magnetic field, *J Geophys Res (USA)*, 84 (1979) 5797.
- Huang C S, Foster J C & Kelley M C, Long duration penetration of the interplanetary electric fields to the low latitude ionosphere during the main phase of magnetic storms, *J Geophys Res (USA)*, 78 (2005) A11309.
- Huang C S & Chen M Q, Formation of maximum electric potential at the geomagnetic equator by the disturbance dynamo, *J Geophys Res (USA)*, 113 (2008) A03301.
- Kikuchi T, Hashimoto K & Nozaki K, Penetration electric fields to the equator during geomagnetic storm, *J Geophys Res (USA)*, 113 (2008) A06214.
- Maruyama N, Sazykin S, Spiro R W, Anderson D, Anghel A, Wolf R A, Toffoletto F R, Rowell T J F, Codrescu M V, Richmond A D & Millward G H, Modelling storm time electrodynamics of the low latitude ionosphere thermosphere system: Can long lasting disturbance electric fields be accounted for?, *J Atmos Terr Phys (UK)*, 69 (2007) 1182.
- Balogh A, Gosling J T, Jokipi J R, Kallenbach R & Kunow H, Corotating interaction regions, *Space Sci Rev (Netherlands)*, 89 (1999) 141.
- Sheeley Jr N R, Harvey J W & Feldman W C, Coronal holes, solar wind streams and recurrent geomagnetic disturbances, *Sol Phys (Netherlands)*, 49 (1976) 271.
- Zhang J, Liemohn M W, Kozyra J U, Thomsen M F, Elliott H A & Weygand J M, A statistical comparison of solar wind sources of moderate and intense geomagnetic storms at solar minimum and maximum, *J Geophys Res (USA)*, 111 (2006) A011065.
- Tsurutani B T, Gonzalez W D, Alicia L, Gonzalez C, Tang F, Arballo J K & Okada M, Interplanetary origin of geomagnetic activity in the declining phase of the solar cycle, *J Geophys Res (USA)*, 100 (1995) 21717.
- Mendillo M & Schatten K, Influence of solar sector boundaries on ionospheric variability, *J Geophys Res (USA)*, 88 (1983) A11 pp 9145–9153.
- Tsurutani B T & Gonzalez W D, The cause of high intensity long duration continuous AE activity (HILDCAAs): Interplanetary Alfvén wave trains, *Planet Space Sci (UK)*, 35 (1987) 405.
- Tsurutani B T, Gonzalez W D, Guarnieri F, Kamide Y, Zhou X & Arballo J K, Are high intensity long duration continuous AE activity (HILDCAA) events substorm expansion events?, *J Atmos Terr Phys (UK)*, 66 (2004) 167.
- Tsurutani B T, Gonzalez W D, Gonzalez A L C, Guarnieri F L, Gopalswamy N, Grande M, Kamide Y, Kasahara Y, Lu G, Mann I, McPherron R, Soraas F & Vasyliunas V, Corotating solar wind streams and recurrent geomagnetic activity: A review, *J Geophys Res (USA)*, 111 (2006a) A011273.
- Tsurutani B T, Mannucci A J, Ijima B A, Komjathy A, Saito A, Tsuda T, Verkhoglyadova O P, Gonzalez W D & Guarnieri F L, Dayside ionospheric (GPS) response to

- corotating solar wind streams, in *Recurrent magnetic storms: Corotating solar wind streams*, Geophys Monogr Ser 167 (AGU, Washington D C), 2006b, pp 245-270.
26. Richardson I G, Energetic particles and corotating interaction regions in the solar wind, *Space Sci Rev (Netherlands)*, 111 (2004) pp 267-376
 27. Tulasi Ram S, Liu C H & Su S Y, Periodic Solar wind forcing due to recurrent coronal holes during 1996-2009 and its impact on earth's geomagnetic and ionospheric properties during the extreme solar minimum, *J Geophys Res (USA)*, 115 (2010) A12340.
 28. Lei J, Thayer J P, Forbes J M, Sutton E K & Nerem R S, Rotating solar CHs and periodic modulation of the upper atmosphere, *Geophys Res Lett (USA)*, 35 (2008a) L10109, doi: 10.1029/2008GL033875.
 29. Thayer J P, Lei J, Forbes J M, Sutton E K & Nerem R S, Thermospheric density oscillations due to periodic solar wind high speed streams, *J Geophys Res (USA)*, 113 (2008) A06307, doi: 10.1029/2008JA013190.
 30. Sobral J H A, Abdu M A, Gonzalez W D, Gonzalez A C, Tsurutani B T, da Silva R R L, Barbosa I G, Arruda D C S, Denardini C M, Zamluti C J & Guarnieri F, Equatorial ionospheric responses to high intensity long duration auroral electrojet activity (HILDCAA), *J Geophys Res (USA)*, 111 (2006) A011393.
 31. Verkhoglyadova O P, Tsurutani B T, Mannucci A J, Mlynchak M G, Hunt L A, Komjathy A & Runge T, Ionospheric VTEC and thermospheric infrared emission dynamics during corotating interaction region and high speed stream intervals at solar minimum: 25 March to 26 April 2008, *J Geophys Res (USA)*, 116 (2011) A09325.
 32. Tsurutani B T *et al.*, Corotating solar wind streams and recurrent geomagnetic activity: A review, *J Geophys Res (USA)*, 111 (2006) A07S01, doi: 10.1029/2005JA011273.
 33. Tsurutani B T, Ho C M, Smith E J, Neugebauer M, Goldstein B E, Mok J S, Arballo J K, Balogh A, Southwood D J & Feldman W C, The relationship between interplanetary discontinuities and Alfvén waves: Ulysses observations, *Geophys Res Lett (USA)*, 21 (1994) 2267.
 34. Huang C S, Sazykin S, Chau J L, Maruyama N & Kelly M C, Penetration electric fields :efficiency and characteristics time scale, *J Atmos Terr Phys (UK)*, 69 (2007) pp 1135-1146.
 35. Nishida A, Iwasaki N & Nagata T, The origin of fluctuations in the equatorial electrojet: A new type of geomagnetic variation, *Ann Geophys (Germany)*, 22 (1966) pp 478-484.
 36. Veenadhari B, Alex S, Kikuchi T, Shinbori A, Singh R & Chandrashekar E, Penetration of magnetospheric electric fields to the equator and their effects on low latitude ionosphere during intense geomagnetic storms, *J Geophys Res (USA)*, 115 (2010) A03305.
 37. Sastri J, Jyoti N, Somyajulu V, Chandra H & Devasia C, Ionospheric storm of early November 1993 in the Indian equatorial region, *J Geophys Res (USA)*, 105 (2000) A8.
 38. Abdu M A, Sobral J H A, de Paula E R & Batista I S, Magnetospheric disturbance effects on the equatorial ionization anomaly (EIA): An overview, *J Atmos Terr Phys (UK)*, 53 (1991) pp 757-771.
 39. Sobral J H A, Abdu M A, Yamashita C S, Gonzalez W D, Gonzales A C, de Batista I S, Zamlutti C J & Tsurutani B T, Responses of the low-latitude ionosphere to very intense geomagnetic storms, *J Atmos Terr Phys (UK)*, 63 (2001) pp 965-974.